Lattice dynamics of some spin-crossover complexes: Mossbauer and VTFTIR measurements

1989 J. Phys.: Condens. Matter 1 7103

(http://iopscience.iop.org/0953-8984/1/39/022)

J. Phys.: Condens. Matter 1 (1989) 7103–7112. Printed in the UK

Lattice dynamics of some spin-crossover complexes: Mössbauer and VTFTIR measurements

A A Yousif†, H Winkler‡, H Toftlund§, A X Trautwein‡ and R H Herber‖

† Physics Department, Sultan Qaboos University, Box 32486, Al-Khod, Sultanate of Oman

‡ Institute of Physics, Lübeck Medical University, Lübeck, Federal Republic of Germany

§ Department of Chemistry, University of Odense, Odense, Denmark

‖ Department of Chemistry, Rutgers University, New Brunswick, NJ, USA

Received 4 January 1989, in final form 21 February 1989

Abstract. Temperature-dependent Mössbauer spectroscopy and variable temperature Fourier transform infrared techniques were employed to follow the spin conversion of Fe(BPTN)$(NCS)_2$ and Fe(TPA)$(NCS)_2$ complexes. The hyperfine interaction parameters and Debye–Waller factors were determined using the Mössbauer effect. The complexes show gradual HS $\rightleftharpoons$ LS transition in the temperature range 4.2–300 K. The lattice dynamical properties at the metal sites in the $^1A_1$ state were observed to be significantly different from those in the $^5T_2$ configuration. It has been demonstrated that detailed *f*-factor measurements may be essential for accurate estimation of the spin-conversion function of such complexes.

1. Introduction

The phenomenon of spin conversion in compounds of the first transition metal series with electronic configuration d^4 to d^7 has been extensively studied and well documented in the literature [1–5]. A variety of physical techniques has been used to observe and follow quantitatively the transition; e.g. magnetic susceptibility, x-ray diffraction, heat capacity, vibrational and optical spectroscopy. In particular, Mössbauer spectroscopy has been especially effective for examining transitions in the iron(II) and iron(III) spin-crossover compounds.

Thermally induced high-spin–low-spin (HS–LS) transitions have been studied in various systems of the [Fe(II)–N_6]-type. Such transitions may be either sudden, with complete conversion from one form to the other within a few degrees, as in the case of Fe(PHEN)$_2$$(NCS)_2$ and Fe(BIPY)$_2$$(NCS)_2$ [6, 7], or much more sluggish, with a gradual conversion extending over a wide temperature range as in Fe(BIPY)$(NCS)_2$ [8].

The Mössbauer effect technique has also been employed to investigate the lattice dynamical properties of some spin-crossover complexes, and a discontinuity of the *f*-factor was observed at the transition temperature [9–13]. Recently, detailed studies on the lattice dynamical behaviour of some complexes, where the Fe(II) ion octahedrally coordinated with N atoms, have revealed that the bonding characteristics and phonon spectra at the Mössbauer atom in the high-spin state are different from those in the low-spin state [14]. The Debye–Waller factors of the respective spin states were derived and

0953-8984/89/397103 + 10 $02.50

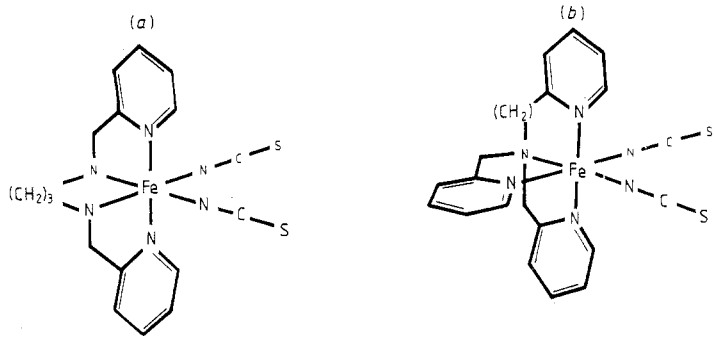

Figure 1. Chemical structure of the spin-crossover complexes investigated. (*a*) Fe(BPTN)$(NCS)_2$; (*b*) Fe(TPA)$(NCS)_2$.

the spin conversion function was calculated from the molar fraction using the measured fractional area. The qualitative features of the function calculated from either the fractional area or the molar fraction may remain the same, especially in complexes with sudden transition. However, in slow transitions, it may be necessary to calculate the function from the molar fraction. The function could deviate considerably from that obtained using fractional area depending on the degree of slowness of the transition, the transition temperature and the magnitudes of the *f*-factors in the distinct spin states. These deviations may manifest themselves quantitatively in a shifted transition temperature and/or inaccurate estimations of the amount of a certain spin state being trapped in the other state in the high- or low-temperature limit. In the present study we report investigations on two spin-crossover complexes, which exhibit slow transition, in an attempt to elucidate some of the features discussed above.

2. Experimental procedure

2.1. Materials

The complexes Fe(BPTN)$(NCS)_2$ [I] and Fe(TPA)$(NCS)_2$ [II] were prepared by reacting iron thiocyanate with the ligands bis(2-pyridylmethyl)trimethylenediamine (BPTN), and tris(2-pyridylmethyl)amine (TPA), respectively. The ligands were earlier prepared by a modified Anderegg method [15]. The reaction takes place under nitrogen atmosphere with the thiocyanate in water and the ligands in ethanol. The end results of the syntheses gave a green Fe(BPTN)$(NCS)_2$ and yellow Fe(TPA)$(NCS)_2$ as described in [16]. The samples were characterised using analytical methods and the chemical structure is given in figure 1.

2.2. Measurements

2.2.1. Variable temperature Fourier transform infrared. The infrared spectra of the Fe(BPTN)$(NCS)_2$ over the temperature range 6–300 K were obtained using a low-temperature cell and an IBM/32 FTIR nitrogen-purged spectrometer. The 300 K data of

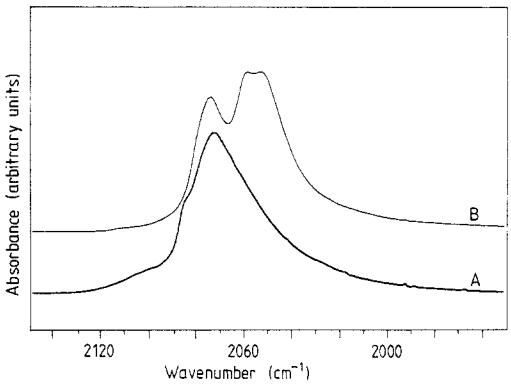

Figure 2. Overlay of IR spectra of Fe(BPTN)$(NCS)_2$ [I] (curve A) and Fe(TPA)$(NCS)_2$ [II] (curve B) at 300 K.

the complexes, summarised in figure 2, were acquired using a Mattson Cygnus-100 spectrometer and subjected to a second-derivative deconvolution procedure. Absorption maxima were located either from this procedure (Cygnus) or by using the PEAKPICK software (IBM), and are reliable to ± 1 cm^{-1} at a nominal instrument resolution of 2 cm^{-1}. The IR data on the Fe(TPA)$(NCS)_2$ complex have been reported earlier [16].

A light-induced excited spin state trapping experiment was performed on the Fe(BPTN)$(NCS)_2$ complex at 6 K. Optical pumping was done by irradiating the sample with either He/Ne 632 nm light or white light from an external incandescent (tungsten filament) light source through a fibre-optic cable. The length of time of irradiation was controlled by the interposition of an absolute shutter between the source and the admittance end of the fibre-optic cable.

2.2.2. Mössbauer spectroscopy. The Mössbauer effect measurements in the temperature range 4.2–300 K were done using a conventional constant acceleration spectrometer in the transmission mode and a liquid helium cryostat. A temperature controller was used to control the temperature to ± 1 K during the period of data accumulation. The Mössbauer spectra were analysed using a non-linear least-squares fitting technique.

The isomer shift and quadrupole splitting Mössbauer parameters are used to characterise the spin state of the resonant atom, while the Debye–Waller factor, f, and its temperature dependence yield information about the lattice dynamical properties of the solid state. The temperature dependence of the f-factor is accurately reflected in the temperature dependence of the area (A) under the resonance curve. For optically thin absorbers, the Mössbauer lattice temperature may be calculated using the Debye model in the high-temperature limit ($T \geqslant \theta_M$) from the relationship

$$d(\ln f)/dT = d\{\ln[A(T)/A(80)]\}/dT = -3E_\gamma^2/Mc^2k_B\theta_M^2. \quad (1)$$

To effect intersample comparison; the area under the resonance curve has been normalised to that at 80 K. In (1) E_γ is the Mössbauer transition temperature, k_B Boltzmann constant and c the velocity of light. The vibrating mass, M, has been taken as that of the 'bare' atom. From the measured values of θ_M, one can calculate the f-factor at a certain temperature T using the relationship

$$f = \exp[-3E_\gamma^2 T/k_B Mc^2\theta_M^2]. \quad (2)$$

The molar population may thus be calculated using the derived f-factor and the measured area.

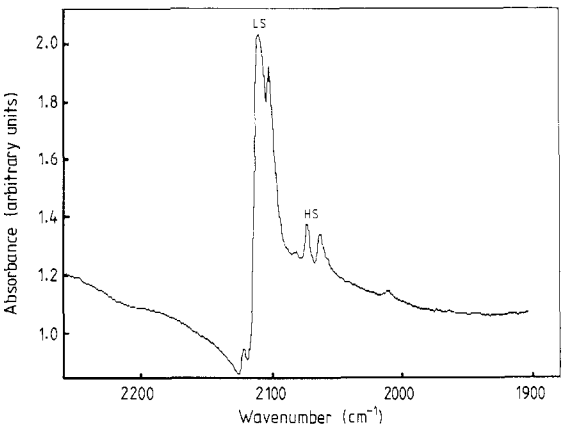

Figure 3. Infrared absorption of spectrum of Fe(BPTN)$(NCS)_2$ in the CN stretching region recorded at 79 K.

Information about the strength of the interatomic bonding forces may be provided from the temperature dependence of the isomer shift. We define an effective vibrating mass, M_{eff}, which gives a qualitative estimate of the chemical bonding of the resonant atom to the lattice. M_{eff} can be calculated using [17]

$$\text{d(IS)}/\text{d}T = -3E_\gamma k_B/M_{\text{eff}}c^2. \tag{3}$$

3. Results and discussion

3.1. VTFTIR measurements

The IR spectrum of Fe(BPTN)$(NCS)_2$ at room temperature, both for the Kel-F (fluorinated grease) mulled and the KBr pelleted sample shows the presence of (mostly) HS form (at 2074 cm^{-1}) with a small amount of LS ($\simeq$2100 cm^{-1}), with the two CN stretching frequencies unresolved. On going to liquid nitrogen temperature both the high-spin form (at 2072 and 2067 cm^{-1}) and the low-spin form (at 2109 and 2101 cm^{-1}) CN stretches are clearly resolved (figure 3). The CS stretch is at about 805 cm^{-1} in the KBr sample (not observable in the Kel-F mulled sample) and the NCS bend is at 476 cm^{-1}, both measured at 78 K.

The temperature dependence of the absorbance difference of LS and HS forms is shown in figure 4. The transition appears to be relatively sluggish, with a transition temperature at about 170 K. At 300 K there may be a small amount of low-spin form present; in any case, the intensity curve has not reached a true 'high-temperature' limit. At 6 K, there is a small amount (estimated in these experiments to be about 8%) of HS form trapped in the LS matrix.

The IR spectrum of Fe(TPA)$(NCS)_2$ at 300 K shows only the HS form and is similar to that of Fe(BPTN)$(NCS)_2$. The splitting at 2053 cm^{-1} band is observed only in KBr. The band positions are calculated from a Gaussian envelope routine. The liquid nitrogen spectrum gives resolved peaks at 2086 and 2062 cm^{-1} which are characteristic of the $^5T_2$ state and other lines at 2122 and 2095 cm^{-1} which are taken as those of the $^1A_1$ ground state. The transition was slow and characterised by the coexistence of high-spin and low-spin ground state around and below the transition temperature [16].

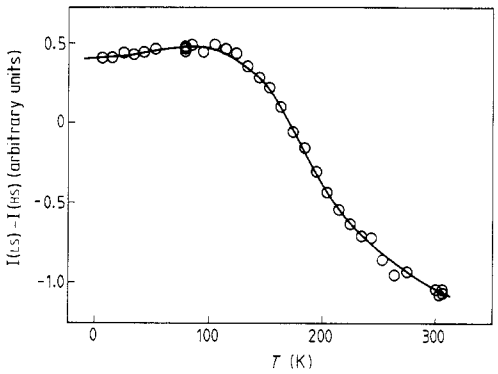

Figure 4. Temperature dependence of absorbance difference for the LS − HS forms of $Fe(BPTN)(NCS)_2$.

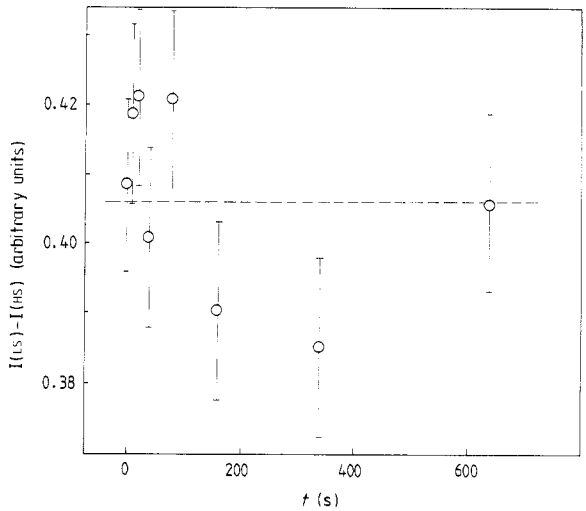

Figure 5. Conversion of the LS to (trapped) HS form of $Fe(BPTN)(NCS)_2$ as a function of time under the influence of white light irradiation at 6 K. Broken line is 0.408 ± 0.013.

We have tried a light-induced excited spin-state trapping (LIESST) experiment on $Fe(BPTN)(NCS)_2$. The complex does not pump optically at 6 K either with He/Ne 632 nm light or with white light. We see *no* conversion within 640 seconds of illumination, under conditions where other complexes of Fe(II) are more than 90% converted to the trapped HS form [17, 18]. Figure 5 gives a plot of the conversion of the LS form to the trapped LS form as a function of time after illumination with white light at 6 K.

3.2. Mössbauer measurements

The hyperfine interaction parameters deduced from the fittings of the Mössbauer spectra of the complexes [I] and [II] in the temperature range 4.2–300 K reveal the coexistence of the high-spin and low-spin iron(II) doublets. Typical values of the fitted parameters at 4.2 K are given in table 1.

The Mössbauer spectrum of $Fe(BPTN)(NCS)_2$ at 4.2 K is found mainly in the LS ground state, with a relative area of 12% in the HS form. At 300 K the complex only partially converted to high spin and about 15% of the area exists in the LS form. Using the fractional area of the respective spin state, a gradual HS $\rightleftharpoons$ LS conversion is observed that suggests a transition temperature of $T_c \simeq 190$ K. This value deviates considerably

Table 1. Mössbauer hyperfine interaction parameters at 4.2 K.

Sample	Spin state	δ (mm s^{-1})	ΔE (mm s^{-1})	Γ (mm s^{-1})	A (%)
Fe(BPTN)$(NCS)_2$	High	1.20(2)	2.58(3)	0.35(5)	12(1)
Fe(TPA)$(NCS)_2$	High	1.07(2)	2.40(3)	0.29(5)	52(1)
Fe(BPTN)$(NCS)_2$	Low	0.53(1)	0.29(1)	0.36(1)	88(1)
Fe(TPA)$(NCS)_2$	Low	0.43(1)	0.39(1)	0.27(1)	48(1)

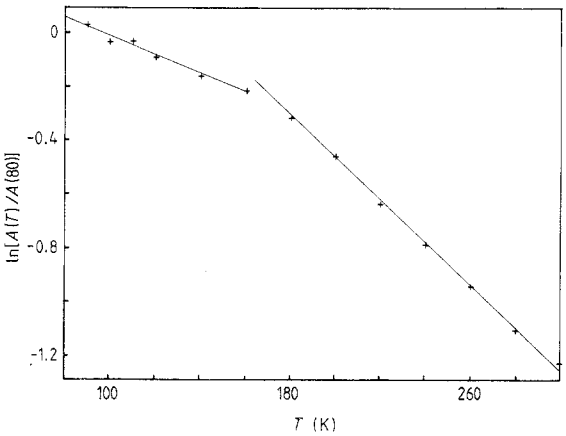

Figure 6. Temperature dependence of the area under the resonance curve in the Fe(BPTN)$(NCS)_2$ complex. The full lines are linear regression fits to the data.

Table 2. Lattice dynamical ^{57}Fe Mössbauer data.

Sample	Spin state	$-\mathrm{d}(\mathrm{IS})/\mathrm{d}T$ (10^{-4} mm s^{-1} K^{-1})	M_{eff} (g mol^{-1})	$-\mathrm{d}(\ln A)/\mathrm{d}T$ (10^{-3} K^{-1})	θ_{M} (K)	f (295 K)
Fe(BPTN)$(NCS)_2$	High	8.34	50(5)	7.51	134(2)	0.10(1)
Fe(TPA)$(NCS)_2$	High	4.69	89(9)	9.87	117(4)	0.05(1)
Fe(BPTN)$(NCS)_2$	Low	1.99	209(20)	3.04	211(2)	0.41(4)
Fe(TPA)$(NCS)_2$	Low	2.51	166(15)	6.20	148(5)	0.16(2)

from the value of T_c = 170 K derived from the VTFTIR and that reported from magnetic susceptibility measurements [19].

The temperature dependence of the total area under the resonance is presented in figure 6 and the data clearly show that the linear dependence of ln A in the lower temperature regime is different from that in the high-temperature region. A linear least square fit of ln A versus temperature was done for $T \geqslant 80$ K for each temperature region separately and respective lattice temperatures were calculated. Since the HS form is preferentially stabilised at high temperatures, a high-spin Mössbauer lattice temperature θ_{M}(HS) was assigned to the high-temperature region. Similarly, a low-spin Mössbauer lattice temperature θ_{M}(LS) was assigned to the lower temperature region. The lattice dynamical parameters derived from the fits of the experimental data are presented in

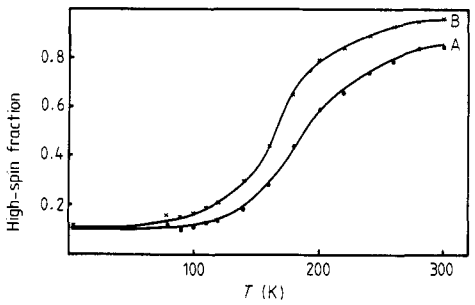

Figure 7. High spin–low spin conversion function of Fe(BPTN)$(NCS)_2$ derived from the fractional area (curve A) or alternatively from the molar fraction (curve B).

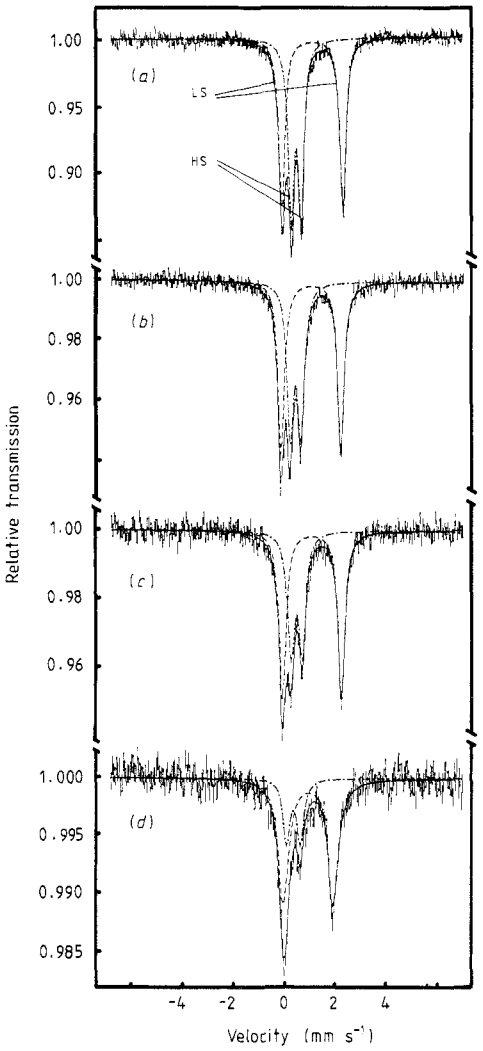

Figure 8. ^{57}Fe Mössbauer spectra of Fe(TPA)$(NCS)_2$ at various temperatures. (*a*) 4.2 K; (*b*) 160 K; (*c*) 180 K; (*d*) 300 K.

table 2. The lattice temperatures allow us to calculate the *f*-factors associated with high-spin (f^{HS}) and low-spin (f^{LS}) states at various temperatures. The spin conversion function is then plotted from the molar fraction using the relationship

$$n(\text{HS})/[n(\text{HS}) + n(\text{LS})] = [A(\text{HS})/f^{\text{HS}}]/[A(\text{HS})/f^{\text{HS}} + A(\text{LS})/f^{\text{LS}}]. \qquad (4)$$

This function now gives a transition temperature $T_c \simeq 170$ K which is consistent with the values obtained from the VTFTIR and magnetic susceptibility measurements. The spin-crossover function, derived from the fractional area or the molar fraction is shown in figure 7. The low-spin population in the high-temperature limit, which appears to be inflated when obtained from the fractional area (15%), is in fact only about 4%. This

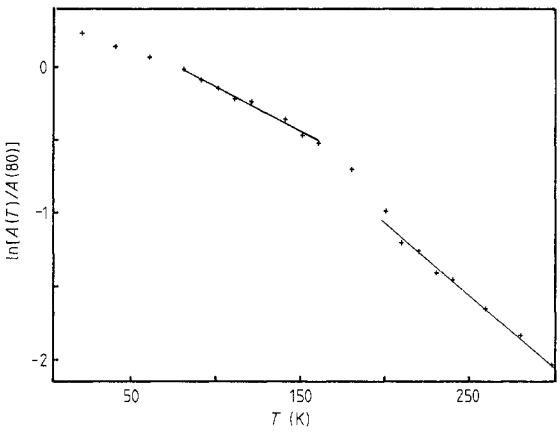

Figure 9. Temperature dependence of the area under the resonance curve in the Fe(TPA)$(NCS)_2$ complex. The full lines are linear regression fits to the data.

strongly supports the VTFTIR data which detect only a small intensity. The amount of HS trapped in the LS matrix derived from the fractional area or molar fraction remains the same (12%) and is in good agreement with the VTFTIR measurements.

The Mössbauer spectra of the Fe(TPA)$(NCS)_2$ show that the complex does not completely convert to LS at 4.2 K or to HS at 300 K. Figure 8 gives representative spectra at various temperatures which tell us that in the region 4.2–160 K, about equal areas of LS and HS doublets were detected. At above 160 K the fractional area of the HS state starts to increase. At room temperature about 25% of LS coexists with the HS.

The Fe(TPA)$(NCS)_2$ was then seen to be a spin-crossover complex according to the IR criterion. In addition, magnetic susceptibility data show a strong temperature-dependent magnetic moment which changes from 2.9 μ_B to 5.4 μ_B in the temperature range 80–300 K [19]. The spin changes are gradual, but residual paramagnetic moments at lower temperatures are relatively high.

We suggest an analysis of the temperature dependence of the total area under the resonant curve, obtained from the Mössbauer spectra, in a similar manner to that performed for Fe(BPTN)$(NCS)_2$. Of course, the presence of appreciable amounts of HS and LS fractions in the whole temperature range (4.2–300 K) will make the analysis incomplete. The qualitative features of the temperature dependence of the total area, shown in figure 9, resemble those of the Fe(BPTN)$(NCS)_2$ and those reported for other spin-crossover complexes [14]; namely, the linear dependence of $\ln A$ in the high-temperature region shows a steeper slope than that in the low-temperature one. But due to the contributions of the LS fraction to the total area in the high-temperature portion, only an upper limit of the Mössbauer lattice temperature, θ_M^{max}(HS), may be derived. Similarly, a lower limit for the lattice temperature of the low-spin state, θ_M^{min}(LS), may be estimated. The respective Debye–Waller factors are calculated from these and the spin-conversion function plotted from the molar fractions, as shown in figure 10. Since f^{LS}/f^{HS} increases with temperature, the LS $\rightleftharpoons$ HS conversion, in fact, starts from 4.2 K as opposed to the apparent spin freezing in the temperature range 4.2–160 K as calculated from the fractional area. Furthermore, the spin conversion is very slow and the complex may be regarded as exhibiting equal populations of LS and HS ground states at 4.2 K. These findings are consistent with the IR and magnetic susceptibility data, and show similarity with the Fe(BIPY)$(NCS)_2$ complex, where a gradual HS $\rightleftharpoons$ LS transition was observed that is qualitatively and quantitatively different from sudden spin transitions observed in other complexes [8, 20].

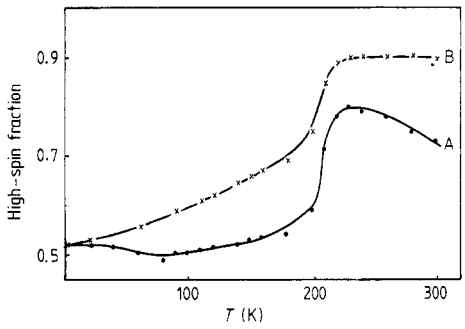

Figure 10. High spin–low spin conversion function of Fe(TPA)$(NCS)_2$ derived from the fractional area (curve A) or alternatively from the molar fraction (curve B).

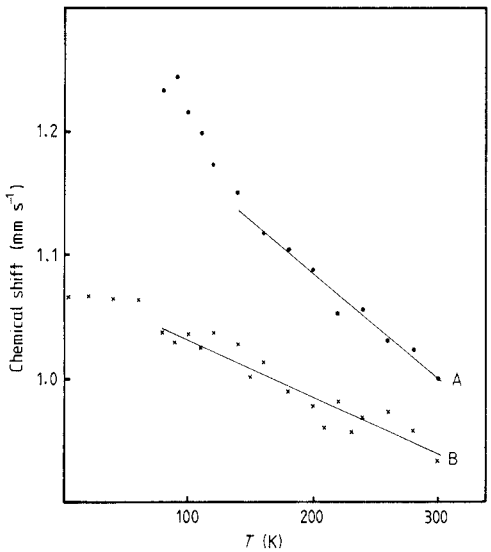

Figure 11. Temperature dependence of the high-spin state isomer shift for complexes [I] (curve A) and [II] (curve B).

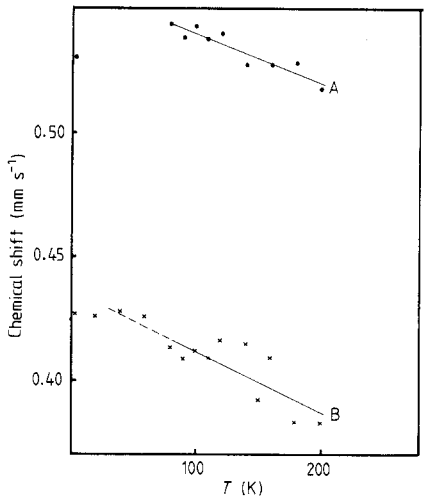

Figure 12. Temperature dependence of the low-spin state isomer shift for the complexes [I] (curve A) and [II] (curve B).

The temperature dependences of the isomer shift in the high-spin state in the complexes [I] and [II] are shown in figure 11, and those in the low-spin ground state in figure 12. A systematic increase of the isomer shift in the Fe(BPTN)$(NCS)_2$ compared with that in Fe(TPA)$(NCS)_2$ reflects the difference in the electron density at the Mössbauer nucleus in the two complexes. The effective vibrating masses of the Mössbauer atoms were derived from the linear fits of the data for $T > 80$ K and presented in table 2. The derived effective masses in the HS and LS forms in the Fe(BPTN)$(NCS)_2$ are different from those in Fe(TPA)$(NCS)_2$ complex, which suggests that the two complexes exhibit different bonding characteristics. Moreover, the results follow the trends observed in other spin-crossover complexes [14]; namely, higher effective masses in the LS ground state than in the HS state. We derive for the low-spin $M_{\text{eff}} = 209$ for [I] and 166 for [II], as compared to the high-spin form of $M_{\text{eff}} = 50$ for [I] and 89 for [II]. These values indicate a stronger metal–ligand bonding in the LS than in the HS form. The transition from the HS to the LS state involves a change in the crystal field splitting energy that may be reflected in the crystallographic parameters and a shorter bond length results in the LS state which

strengthens the bonding interaction. A drastic increase in the intramolecular volume, which results in metal–ligand bond length changes by nearly 10%, has been reported to accompany spin conversion from LS to HS [21]. Consequently, the lattice expands and the elastic properties are different in the two spin states.

References

[1] Martin R H and White A H 1968 *Trans. Met. Chem.* **4** 113
[2] Goodwin H A 1976 *Coord. Chem. Rev.* **18** 293
[3] Gutlich P 1981 *Struct. Bonding* **44** 83
[4] Gutlich P 1984 *Mössbauer Spectroscopy Applied to Chemistry* vol 1 ed. G J Long (New York: Plenum) p 287
[5] Gutlich P 1984 *Chemical Mössbauer Spectroscopy* ed. R H Herber (New York: Plenum) p 27
[6] Konig E, Majeda K and Watson K J 1968 *J. Amer. Chem. Soc.* **90** 1146
[7] Konig E, Ritter G and Kulshreshtra S K 1985 *Chem. Rev.* **85** 219
[8] Dockum B W and Reiff W M 1982 *Inorg. Chem.* **21** 1406
[9] Konig E, Ritter G, Spiering H and Kremer S 1972 *J. Chem. Phys.* **56** 3139
[10] Konig E, Ritter G and Goodwin H A 1973 *Chem. Phys.* **1** 17
[11] Konig E and Ritter G 1973 *Phys. Lett.* A **43** 488
[12] Konig E, Ritter G and Goodwin H A 1974 *Chem. Phys.* **5** 211
[13] Konig E, Ritter G, Irler W, Goodwin H A and Kanellakopulos B J 1977 *Phys. Chem. Solids* **39** 521
[14] Yousif A A and Herber R H 1987 *Hyp. Int.* **36** 13
[15] Andregg G and Wenk F 1967 *Helv. Chim. Acta* **50** 2330
[16] Hojland F, Toftlund H and Yde-Andersen S 1983 *Acta Chem. Scand.* A **37** 251
[17] Herber R H (ed.) 1984 *Chemical Mössbauer Spectroscopy* (New York: Plenum) p 119
[18] Herber R H and Casson L M 1986 *Inorg. Chem.* **25** 847
[19] Toftlund H, Pedersen E and Yde-Andersen S 1984 *Acta Chem. Scand.* A **38** 693
[20] Herber R H 1987 *Inorg. Chem.* **26** 173
[21] Mikami M, Konno M and Saito Y 1979 *Chem. Phys. Lett.* **63** 566